

AN OVERVIEW OF DRAG EMBEDDED ANCHOR HOLDING CAPACITY FOR DREDGING AND OFFSHORE APPLICATIONS

S.A. Miedema¹, G.H.G. Lagers², J. Kerkvliet³

ABSTRACT

Dredging and mining is shifting to deeper waters. For dredging with TSHD's the limit is around 150 m of water depth, but for mining the water depth can be hundreds or even thousands of meters. New technologies have to be developed or copied and adapted from the offshore industry. At the Delft University, Offshore Engineering, students carry out research into many subjects related to moorings and mooring systems, like:

1. The holding capacity of drag anchors in sand.
2. The holding capacity of drag anchors in clay.
3. The holding capacity and operations of suction anchors.
4. The use of the catenary equation in moorings.
5. The methodology about choosing the right anchor for different purposes.
6. The methodology about choosing the right anchor line for different purposes and conditions.
7. The methodology about designing an anchoring system for FPSO's.
8. The methodology about designing an anchoring system for SPAR's.
9. The methodology about designing an anchoring system for Semi-Sub's.

The results of the research can also be found on: <http://www.offshoreengineering.org>. In dredging and offshore anchors are used for positioning, but also for operations (the cutter suction dredger). In all cases it is evitable that a proper estimation of the holding capacity is very useful when designing the application.

The holding capacity of anchors depends on the digging depth, the soil mechanical properties end of course the dimensions and the shape of the anchor. The digging depth also depends on the soil mechanical properties and the shape of the anchor. Now the first question is of course how is the digging depth related to the soil mechanical properties and the shape of the anchor and the second question is, how does this relate to the holding capacity.

By means of deriving the equilibrium equations of motion of the anchor and applying the cutting theories, the digging behavior of anchors can be simulated. The main challenges are how to model the shape of the anchor and how to apply the existing cutting theories to this complex shape. This paper gives a first attempt to derive equilibrium equations based on the cutting theory of Miedema (1987).

Keywords: Dredging, anchors, holding capacity, soil mechanics

INTRODUCTION

This paper is the result of assignments carried out by students for the Offshore Moorings course of the MSc program Offshore Engineering of the Delft University. In this study an analyses is made of the penetration behavior of an anchor in sand. The following points are to be taken into account.

- The geometry of the anchor and how to simplify it.
- What happens when the anchor penetrates the soil?
- Which forces will occur during penetration?
- How to solve this mathematically?

First of all, the most common anchors on the market are analyzed and a general anchor geometry will be chosen. This chosen geometry will be simplified to a 2D geometry, which will be realistic for a first analysis. After this step the penetration behavior of an anchor will be described in different phases, such a way that it is clear and easy to

¹ Associate Professor, Delft University of Technology, s.a.miedema@3me.tudelft.nl

² Associate Professor, Delft University of Technology, g.h.g.lagers@tudelft.nl

³ Student in Offshore Engineering, Delft University of Technology. JohnKerkvliet@wanadoo.nl

understand. Forces on the soil layer, fluke, shank and mooring line forces will be defined and analyzed. The forces will be described as a function of the geometries including the relevant variable angles.

THE GEOMETRY OF THE ANCHOR

While searching for the best simplified anchor geometry, knowledge of the most common anchors on the market is needed. Vrijhof Anchors 2005 gives a good overview of the most common anchors. Two types of anchors can be considered, horizontal load anchors and vertical load anchors. The vertical load anchor can withstand both horizontal and vertical mooring forces. The horizontal anchor or drag embedment anchor can only resist the horizontal loads. The drag embedment anchor is mainly used for catenary moorings, where the mooring line arrives the seabed horizontally. The vertical load anchor is used in taut leg mooring systems, where the mooring line arrives at a certain angle the seabed. A good starting-point for this case is to analyze the horizontal load anchor, because this anchor is often used and will form an adequate challenge. To determine a simplified geometry of this horizontal anchor an actual figure of this anchor is needed. In the Figures 1 and 2, a sketch of the selected anchor can be found.



Figure 1. Examples of anchors.

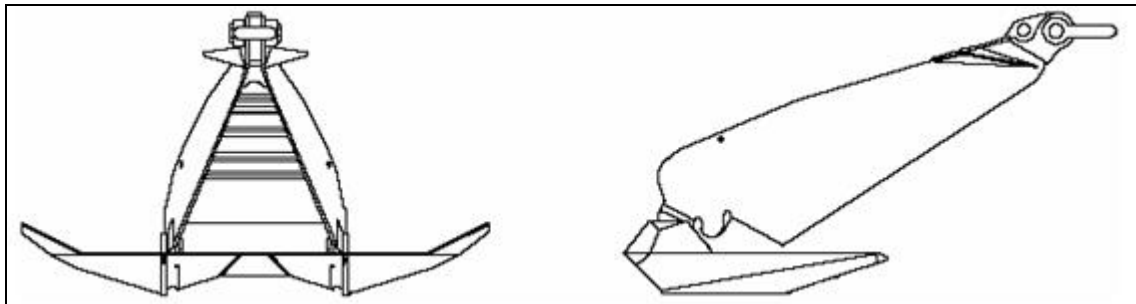


Figure 2. The geometry of anchors.

The actual blade (fluke) on the anchor that will penetrate the soil is represented by the horizontal part of the above given figure. The shank is represented by the other part of the anchor. On the end of the anchor an anchor shackle can be found. A first simplification will be made by modeling the anchor as a 2D model. Hereby all the calculations will be made easier, but the geometry is still too complex to determine all the forces. A second simplification can be made by supposing the anchor as two straight lines as can be seen Figure 3. This simplification is allowed, because this is a conceptual (first) model. When all the forces and the penetration curve of this simple model are known, a much more complicated model can be made. Figure 4 gives an overview of drag embedded anchors.

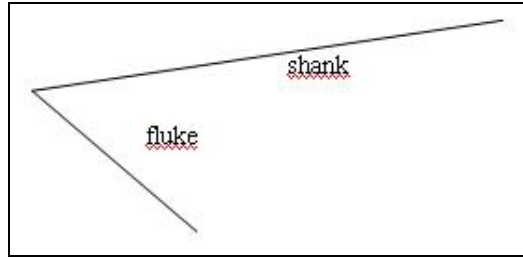


Figure 3. The definition of fluke and shank.

For the rest of the case a few assumptions must be made. First, the type of soil will be sand, this way the cohesion and adhesion effects can be neglected. As a next assumption, it is considered that the anchor penetrates the soil at a very low velocity. Therefore inertia and water tension can also be neglected. Several constrains were also made to simplify the 3D force analysis into a 2D analysis. This way several shear zones can be neglected. As a final assumption, the force acting on the point of the fluke will be neglected. This force is low considering a big anchor and will be fully cancelled by the force perpendicular on the shank.

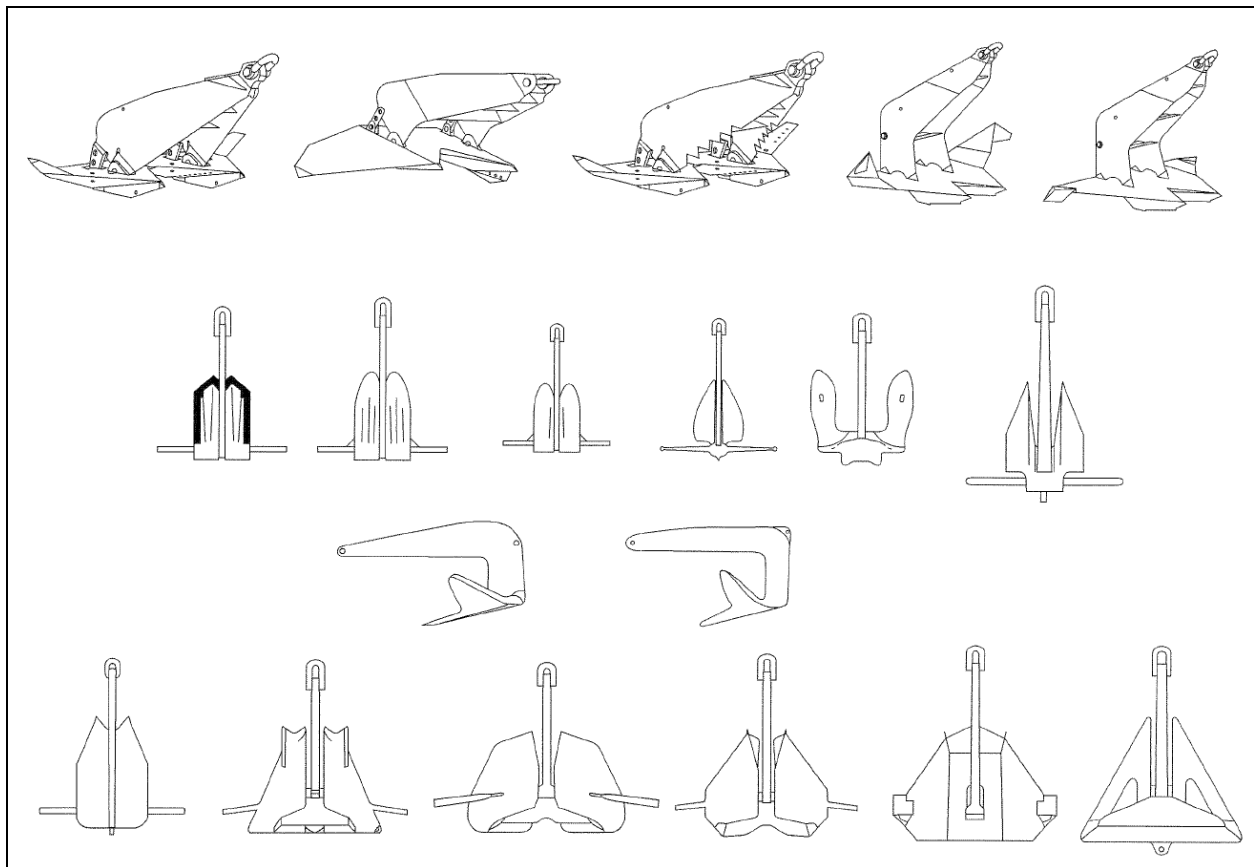


Figure 4. Typical drag embedded anchors (API 2005).

SOIL RESISTANCE TO EMBEDDED ANCHOR LINE

The forces on the embedded anchor line can be seen as a separate system in the anchor burial process and will be treated first. Up until 1989 the work reported on embedded anchor chains was basically theoretical. Values of the design parameters such as the effective chain width in sliding (B_s), the effective chain width in bearing (B_b) and the

bearing capacity factor in clay (N_c) were suggested, but little experimental proof confirmed their validity. With respect to general practice, the effective chain widths can be expressed in terms of the nominal chain diameter (D):

$$B_s = EWS \cdot D \quad (1)$$

$$B_b = EWB \cdot D \quad (2)$$

where EWS and EWB are the parameters to express the effective widths in sliding and bearing, respectively.

Vivatrat et al. (1982) developed the analytical model of a chain inside soil by assuming the chain length inside soil as a summation of short line segments and expressing the equilibrium conditions of each segment. The effective width parameters EWS and EWB proposed were 10 and 2.6, respectively and the use of a value for N_c between 9 and 11 was suggested.

Yen and Tofani (1984) performed laboratory measurements on sliding and bearing soil resistances on a $\frac{3}{4}$ inch diameter stud-link chain in very soft silt. During cutting and sliding tests, the maximum soil resistances were established to be mobilized within a small movement of chain, even less than half a link. The EWS parameter can be determined from laboratory tests and varies between 5.7 and 8.9. The N_c factor at a particular depth was found to be between 7.1 and 12.1, considering the EWB parameter to be 2.37.

Using the finite segment approach, Dutta (1986, 1988) derived the nodal equilibrium equations for chain segments and proposed a simple calculation method. This study showed good agreement with the results obtained by the analytical method used by Vivatrat et al. (1982).

Degenkamp and Dutta (1989) derived a more accurate analytical model of embedded chain under soil resistance and a simple calculation procedure. They used a soil model to accurately predict the soil resistances to the chain inside soil and estimated critical design parameters, such as effective widths of chain, based on laboratory tests.

Assuming: (1) Chain elements are inextensible; (2) due to the chain shift, the soil medium suffers an undrained loading condition; (3) soil in the vicinity of the chain reaches limit state of stress and thereby develops ultimate soil resistances; and (4) the shear strength and weight of the soil over a chain element are constant. The forces on a chain element are as presented in Figure 5.

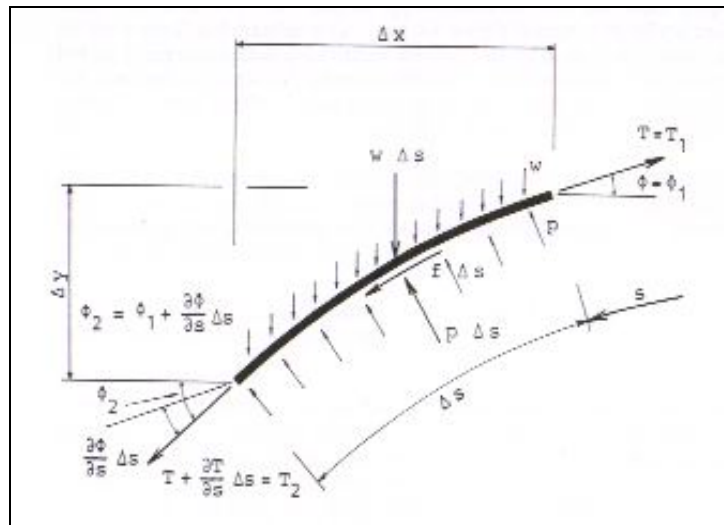


Figure 5. Force system on an embedded anchor line.

Assuming Δs is small, equilibrium in tangential direction leads to:

$$\frac{\partial T}{\partial s} = -(f + w \sin \Phi_1) \quad (3)$$

and by using the incremental integration approach, one can write:

$$T_2 = T_1 - \Delta s(f + w \sin \Phi_1) \quad (4)$$

Equilibrium in normal direction (Δs is small) leads to:

$$\frac{\partial \phi}{\partial s} = \frac{P - w \cos \Phi_1}{T + \frac{\partial T}{\partial s} \Delta s} \quad (5)$$

or, for discrete elements, applying the incremental approach:

$$\Phi_2 = \Phi_1 + \frac{(p - w \cos \Phi_1) \Delta s}{T_2} \quad (6)$$

The entire embedded chain configuration can be assumed to be a summation of the discrete chain elements. For each element, the value of T_2 and Φ_2 can be determined using the known values of T_1 , Φ_1 , w , f and p . To determine f and p , the tangential movement has been assumed to cause an uncoupled sliding resistance, independent of the normal soil resistances. Using this assumption, the frictional resistance is written as:

$$f = B_s \alpha S_u \quad (7)$$

And the normal soil resistance is written as:

$$p = B_b q \quad (8)$$

The value of q is evaluated using the formula given by Skempton (1951) for the ultimate net soil resistance of a strip footing:

$$q = N_c S_u \quad \text{Where } N_c = 5.14 \left(1 + 0.2 \frac{h}{B_b} \right) \quad (\text{with a maximum } N_c = 7.6) \quad (9)$$

From these equations, it can be seen that the accuracy of p and f are governed by the factors ($EWB \times N_c$) and ($EWS \times \alpha$) respectively. Extensive testing led to the next values:

- For very soft ($S_u = 5$ kPa) clay: $EWB = 2.5$, $EWS = 8.0$
- For firm ($S_u = 34$ kPa) clay: $EWB = 2.3$, $EWS = 7.2$

Grote (1993) used the exact same approach and values obtained by Degenkamp and Dutta (1989) to determine the force distribution and geometric profile of the embedded anchor line in his work to simulate the kinematic behavior of work anchors.

Neubecker and Randolph (1994, 1995) derived closed form expressions for both the load development and chain profile to avoid the numerical solution by an incremental integration technique used by Degenkamp and Dutta (1989) and simplify the procedure. Their work corroborates the results found by Degenkamp and Dutta. For the typical case where the chain angle at the seabed is zero, the expression becomes:

$$\frac{T_a \theta_a^2}{2} = D\bar{Q} \quad (10)$$

The expression for frictional development along the chain was derived as:

$$\frac{T_0}{T_a} = e^{\mu\theta_a} \quad (11)$$

In addition they found formulations for the embedded anchor line in sand using the same approach, but changing the bearing capacity factor. For non-cohesive soils, the bearing pressure q may be expressed in terms of a standard bearing-capacity factor N_q as:

$$q = N_q \gamma' z \quad (12)$$

THE KINEMATIC BEHAVIOR OF DRAG ANCHORS IN CLAY

Grote (1993) derived a dynamic model to describe the anchor embedment. He described the forces on the anchor as illustrated in Figure 6. The forces on the anchor consist of its weight, shear and normal forces on both fluke and shank and the tension force from the anchor line pulling the anchor. The fluke force ff is calculated with a transformation of the cutting formula of Miedema 1987. Grote states that the force on the fluke depends on the depth and velocity of the anchor and a constant, containing soil specific properties. This leads to a quantitative formula of this force:

$$ff = C(\text{depth})^a (\text{velocity})^b \quad (13)$$

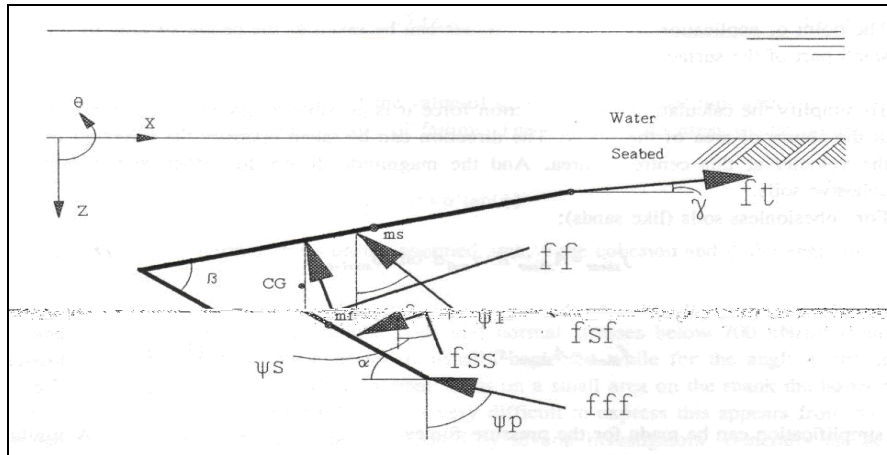


Figure 6. Forces on an embedded anchor.

The second force on the fluke, fff , is a front force on the fluke caused by the bearing capacity of the surrounding soil. This same force is present at the shank of the anchor and called fsf . They are both calculated with the formula for the bearing resistance of a strip footing formulated by Terzaghi:

$$fff = fsf = A_{\text{front}} \left(cN_c + \frac{\gamma B}{2} N_\gamma + \gamma d N_q \right) \quad (14)$$

For no free-draining soils as clay, it can be assumed that the internal friction angle $\phi = 0$ and $N_q = 1$. The second term is small compared to the last one, so equation 16 can be simplified to:

$$fff = fsf = A_{\text{front}} (cN_c + \gamma d) \quad (15)$$

f_{ss} is a shear force on the shank. In clay ground the angle of internal friction is assumed zero while the cohesion is not. The shear stress where failure occurs is then equal to the cohesion, which is equal to the undrained shear strength.

$$f_{ss} = A_{\text{shear}} s_u \quad (16)$$

And finally, f_t is the force on the pad eye implied by the anchor line.

Steward (1992) published methods to describe the kinematic behavior of drag anchors in cohesive soils. These methods were simplified by Neubecker and Randolph (1995) who formulated bearing capacity and moment equilibrium calculations utilizing two fundamental anchor resistance parameters, f and θ_w . The assumption that a drag anchor travels parallel to its flukes is widely accepted. Therefore the authors expressed a geotechnical resistance force T_p acting on the anchor parallel to the direction of the fluke, illustrated in Figure 7, as:

$$T_p = f A_p N_c s_u \quad (17)$$

Since there will also be geotechnical forces normal to the fluke, the resultant resistance force T_w acting on the anchor will make an angle θ_w with the fluke.

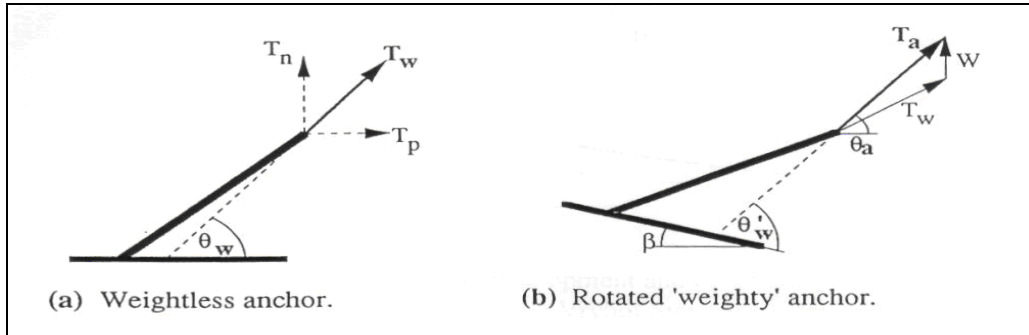


Figure 7: anchor parameter, θ_w

Therefore:

$$T_w = \frac{T_p}{\cos \theta_w} \quad (18)$$

The pad eye force T_a can be determined as the resultant of T_w and the anchor weight W_a . As the anchor embeds, the upper fluke surface and resultant force T_a will be at angles of β and θ_a respectively to the horizontal. Allowing for the offset angle ψ between T_w and T_a , it then follows that:

$$\beta = \theta_w + \psi - \theta_a \quad (19)$$

Neubecker and Randolph (1994, 1995) also developed an expression for the anchor chain tension and angle at the anchor padeye assuming the chain angle at the seabed is zero:

$$\frac{T_a \theta_a^2}{2} = D \bar{Q} \quad (20)$$

Every anchor can be considered to have unique properties f and θ_w that are independent of the anchor size or the soil strength profile, and can be determined by experimental modeling or comparison against published field data. The equations described above can then be implemented into an incremental simulation as follows:

1. Assume an anchor fluke orientation β and displace the padeye horizontally an increment Δx .
2. Calculate the new embedment depth D , assuming motion parallel to the previous fluke orientation.
3. Calculate the anchor resistance T_a from the anchor characteristics, anchor orientation and local soil strength.
4. Calculate the chain angle θ_a using equation 20.
5. Calculate the new fluke angle β using equation 19 in order to maintain equilibrium.
6. Displace the padeye a further increment Δx and loop to step 2.

By adjusting the variables involved, the authors showed agreement with centrifuge and full-scale tests.

Thorne 1998 developed a theory from geotechnical principals, without the use of any site or anchor specific correlations. His predictions of the anchor movement showed good agreement with nine full scale tests covering three different sites and five anchor types. The equations used are based on the proposition that no movement will occur until the soil forces acting parallel to the fluke are overcome. The motion of the anchor results in the soil around the shank failing in bearing capacity on the underside and in shearing on the base and sides, exerting on the shank the maximum force of which the soil is capable. This is also true for other elements which have to be dragged through the soil like shackles, palms and stabilizers. These forces are calculated as:

$$\text{Drag} = DA_i DF_i S_u \quad (21)$$

where DA_i and DF_i are the area and drag factor for the “ith” component, acting at an angle α_i to the plane of the fluke on the anchor element (Figure 8).

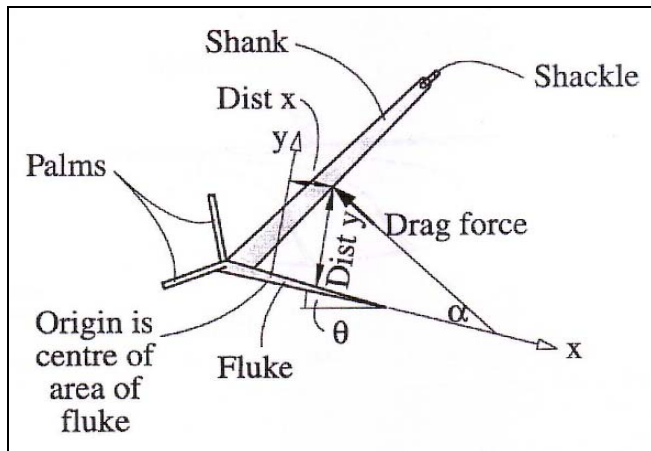


Figure 8. The anchor model.

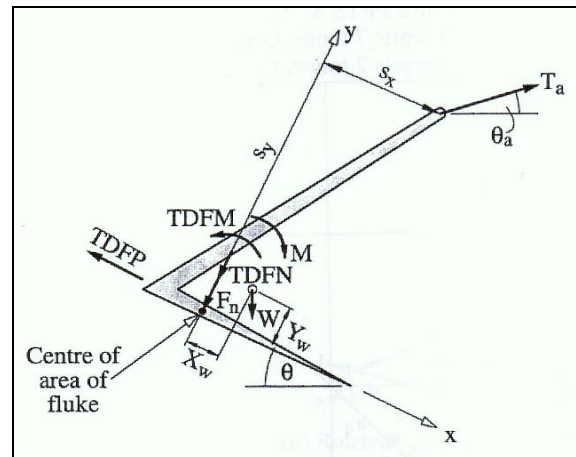


Figure 9. The force application points.

There are three drag components: base bearing and skin adhesion of the base (acting at right angles to the element), and skin adhesion on the sides (acting parallel to the fluke). The drag factors are shape dependant and taken from geotechnical research on soil forces on cylinders, flat plates, wedges and strip footings. All forces are assumed to act at the centers of the respective areas and the undrained shear strength is taken as that at the centre of area. The forces of each element can be added to give the total drag force components normal and parallel to the fluke and the moments about the fluke centre of area:

$$TDFN = \sum_{i=1}^{i=n} -DA_i DF_i S_u \sin \alpha_i \quad (22)$$

$$TDFM = DA_f DF_f S_u + \sum_{i=1}^{i=n} DA_i DF_i S_u \cos \alpha_i \quad (23)$$

$$\text{TDFM} = \sum_{i=1}^{i=n} \text{DA}_i \text{DF}_i \text{S}_u (\text{Dist}x_i \sin \alpha_i + \text{Dist}y_i \cos \alpha_i) \quad (24)$$

Considering an anchor with its fluke at an angle θ to the horizontal, the centre of area of the fluke at a depth D below the seabed and the anchor chain at an angle θ_a to the horizontal (Figure 9), the equilibrium equations are:

$$\text{T}_a \cos(\theta + \theta_a) = \text{TDFP} - \text{W} \sin \theta \quad (25)$$

$$\text{F}_n = \text{T}_a \sin(\theta + \theta_a) - \text{W} \cos \theta - \text{TDFN} \quad (26)$$

$$\text{M} = \text{T}_a \{ \text{S}_x \sin(\theta + \theta_a) - \text{S}_y \cos(\theta + \theta_a) \} + \text{TDFM} - \text{W}(\text{Y}_w \sin \theta + \text{X}_w \cos \theta) \quad (27)$$

To solve this force system with the four unknowns M , T_a , F_n , θ_a , one more equation is needed. Thorne used the closed form expression given by Neubecker and Randolph 1995 for the anchor shackle tension, T_a , and the angle of the chain at the anchor to the horizontal, θ_a :

$$\frac{\text{T}_a \theta_a^2}{2} = \text{DQ} \quad (28)$$

The proposed approach for progressive penetration is based on the pressure distribution over a flat plate. An anchor fluke is considered, B long and L wide, at some position acted upon by a normal force, F_n , and a moment, M , which results in the idealized contact pressure distribution $abcd$ and stress changes as the plate is moved a distance δ_s (Figure 10).

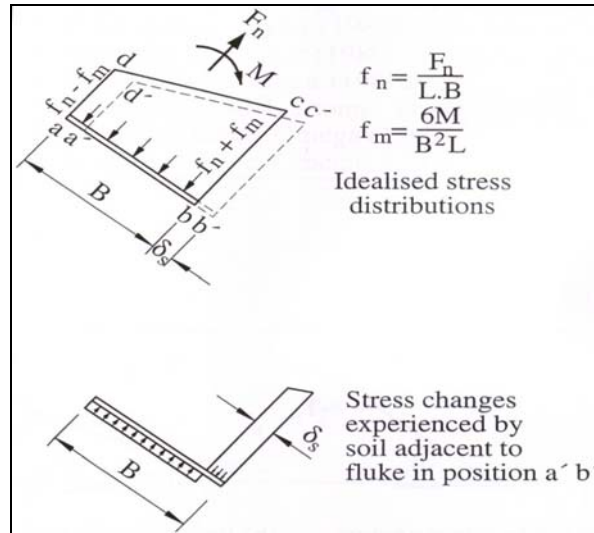


Figure 10. The pressure distribution.

These stress changes can be considered as a loading on the plate consisting of an equivalent normal force and moment acting at the centre of area.

$$\text{F}_{\text{eq}} = \text{L} \left\{ \delta_s \left(f_n + f_m - \frac{f_m \delta_s}{B} \right) - \frac{2f_m \delta_s (B - \delta_s)}{B} \right\} \quad (29)$$

$$\text{M}_{\text{eq}} = \text{L} \left\{ \frac{\delta_s (B - \delta_s)}{2} \left(f_n + f_m - \frac{f_m \delta_s}{B} \right) - \frac{f_m \delta_s^2 (B - \delta_s)}{B} \right\} \quad (30)$$

Now the incremental normal and angular deflections of the fluke after the movement δ_s are assumed to be proportional to F_{eq} and M_{eq} with proportionality constants K_1 and K_2 respectively. K_1 and K_2 are functions of the elastic modulus of the soil, the plate size and the relative depth of the plate. If the plate moves a total distance S parallel to its plane, there will be $\frac{S}{\delta_s}$ increment and the resulting total deflections of the centre of area, δ_n and δ_θ are:

$$\delta_n = K_1 \frac{S}{\delta_s} F_{eq} \stackrel{\delta_s \rightarrow 0}{=} K_1 LSB(f_n - f_m) = K_1 \frac{S}{B} \left(F_n - \frac{6M}{B} \right) \quad (31)$$

$$\delta_\theta = K_2 \frac{S}{\delta_s} M_{eq} \stackrel{\delta_s \rightarrow 0}{=} \frac{K_2 LSB(f_n + f_m)}{2} = K_2 \frac{S}{B} \left(\frac{F_n B}{2} + 3M \right) \quad (32)$$

To allow estimation of the response of a real anchor fluke, an equivalent rectangular fluke is used with the same centre of area and absolute first moment of area. For a rectangle, the values of K_1 and K_2 are based on research done by Lee (1962), Whitman and Rickart (1967), Butterfield and Bannerjee (1971) and Rowe and Davis (1982) on deflection coefficients for a buried plate (Figure 11):



Figure 11. The deflection coefficients for a buried plate.

$$K_1 = I_d \left(\frac{0.6B + 0.3L}{BLE_u E_c} \right) \quad (33)$$

$$K_2 = \frac{I_m I_d}{E_u E_c B^2 L} \quad (34)$$

The term I_m takes account of the aspect ratio of the rectangle, I_d takes account of the depth effect, E_c is a reduction factor to take account for post yield behavior and E_u is the undrained elastic modulus of the soil.

The analysis of progressive movement now proceeds as follows. Assume the fluke moving a distance S , parallel to its plane, from an old position ($n-1$) to a new position n and rotating an angle δ'_θ from the initial angle θ_{n-1} to an angle θ_n . The statics can be solved to find F_n and M for equilibrium. Now using the progressive penetration approach as described above, it is possible to estimate the angular displacement δ_θ which would occur if this combination of F_n and M were applied to the plate. Repeating this for various angular displacements until $\delta_\theta = \delta'_\theta$ will result in the angle θ for this step. The drag distance (horizontal movement), IDD , of the anchor from position $n-1$ to n is then calculated as:

$$IDD = \frac{S \sin \theta_{n-1}}{\tan\left(\frac{\theta_{n-1} + \theta_n}{2}\right)} + \delta_n \sin \theta_n \quad (35)$$

and the new depth for step $n+1$, D_{n+1} , is calculated as below and the whole process is repeated.

$$D_{n+1} = D_n - \delta_n \cos \theta_n + S \sin \theta_n \quad (36)$$

A value of $S = 1.0B$ was adopted for calculation.

Finally the American Petroleum Institute 2005 gives a graph for the holding capacity in soft clay based on the ratio of the weight of the anchor and the holding capacity. This graph is shown in Figure 12, and gives lines for different types of anchors. Of course this graph shows a worst case scenario based on soft clay.

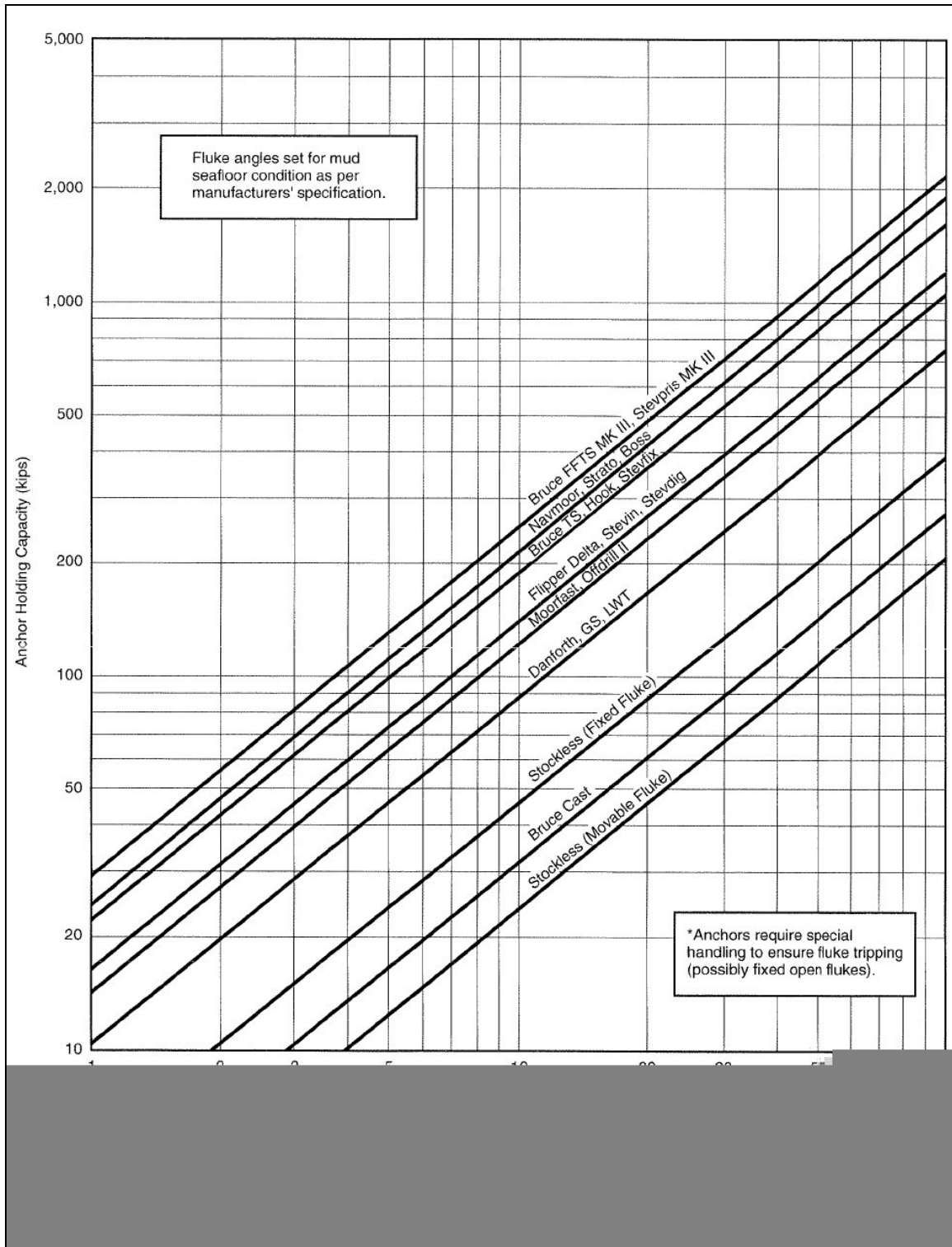


Figure 12. Anchor holding capacity in soft clay (API 2005).

THE KINEMATIC BEHAVIOR OF DRAG ANCHORS IN SAND

Compared to the behavior of an anchor in clay, the weight of the soil above the anchor plays an important role in non cohesive soils like sand.

Le Lievre and Tabatabaee 1981 proposed a limit equilibrium method. This method has been shown to give reasonable predictions of the ultimate holding capacity of drag anchors in sand, for a given depth of embedment. However, several assumptions in the analytical procedure make it unsuitable for application to a drag anchor during embedment, and hence the approach does not allow prediction of the depth to which the anchor will embed, and thus the actual capacity. A schematic representation of the failure mode and force system adopted by Le Lievre and Tabatabaee is shown in Figure 13.

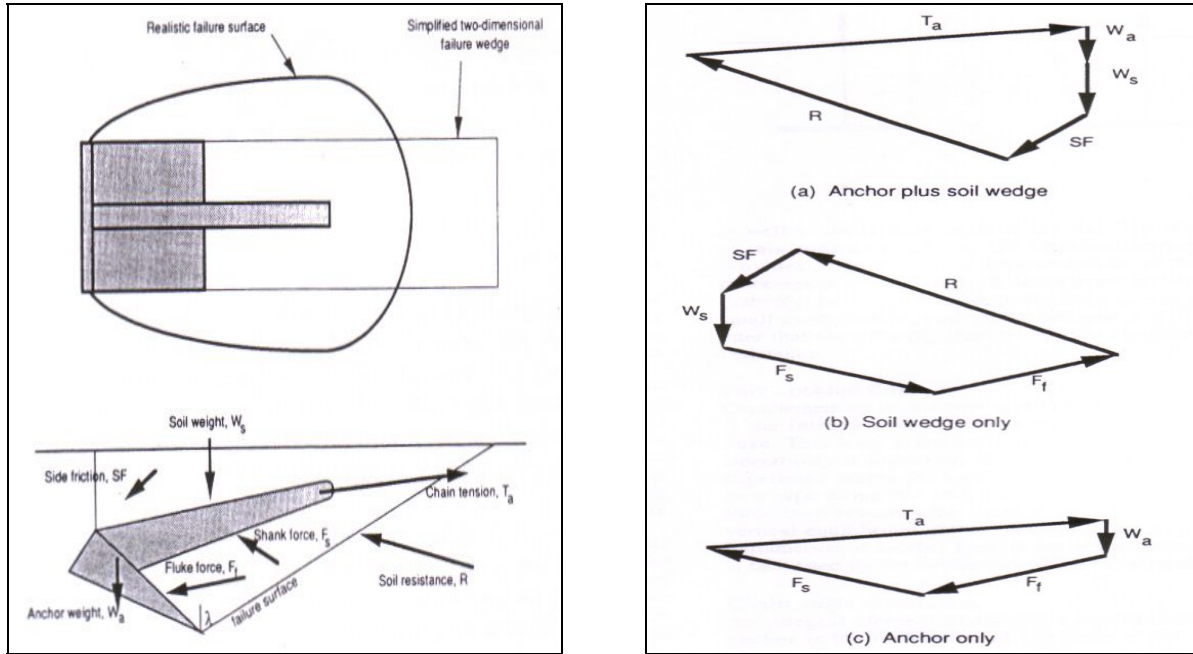


Figure 13. Soil failure mode and force system.

The proposed solution procedure followed in a stepwise manner:

1. Assume a failure wedge angle, λ , of the soil.
2. For the particular failure wedge angle, λ , calculate the mobilized mass of soil, W_s .
3. For the particular failure wedge angle, λ , calculate the side friction, SF. The side friction is assumed to be the force required to overcome the lateral earth force acting on the soil wedge area, hence:

$$SF = \int_{\text{Area}} K_s \gamma z \tan(\phi) dA \quad (36)$$

4. From the force polygon of the soil wedge plus anchor (Figure 13), solve for the two unknowns of chain tension, T_a , and soil reaction, R .
5. From either of the other two force polygons of soil wedge only, solve for the values of shank force, F_s , and fluke force, F_f .
6. Go back to step 1 and repeat with a different value of λ . Stop procedure after minimum chain tension is calculated. This value is the best upper bound solution to the problem.

Grote (1993) defined a force model shown in Figure 10. His problem approach is the same for clay as for sand grounds only the formula's for the ground resistances are different.

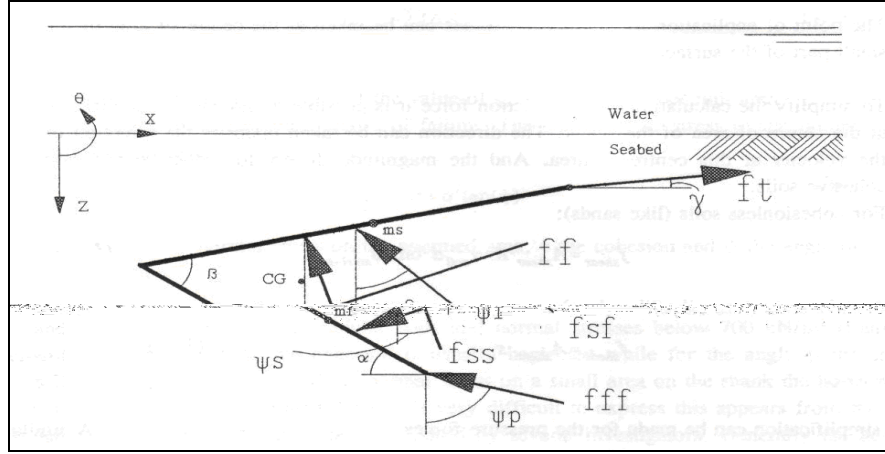


Figure 14. Forces on an embedded anchor.

The fluke force **ff** is calculated with a quantitative formula:

$$\mathbf{ff} = C(\text{depth})^a (\text{velocity})^b \quad (37)$$

The second force on the fluke, **fff**, is a front force on the fluke caused by the bearing capacity of the surrounding soil. This same force is present at the shank of the anchor and called **fsf**. They are both calculated with the formula for the bearing resistance of a strip footing formulated by Terzaghi:

$$\mathbf{fff} = \mathbf{fsf} = A_{\text{front}} \left(cN_c + \frac{\gamma B}{2} N_\gamma + \gamma d N_q \right) \quad (38)$$

where N_c , N_γ and N_q are the bearing capacity factors, c the cohesion of the soil, γ the unit weight of the soil, B the width of the footing (here fluke and shank) and d the depth of the bottom of the footing. For free-draining soils such as sand, the cohesion c is thought to be zero. The second term is small compared to the last one, so equation 38 can be simplified to:

$$\mathbf{fff} = \mathbf{fsf} = A_{\text{front}} (\gamma d N_q) \quad (39)$$

To take account for the under pressure that can occur during anchor burial, the author used a empirical equation which is a combination of the foundation theory of Terzaghi and the cutting theory of Miedema set up by Becker et al. 1992:

$$\mathbf{fff} = \mathbf{fsf} = A_{\text{front}} N_q \left(\gamma_{\text{soil}} \frac{d}{2} + \gamma_{\text{water}} \Delta p \right) \quad (40)$$

where Δp is the pore under pressure that follows from the cutting theory of Miedema.

fss is a shear force on the shank. In sand ground the horizontal stress is assumed to be a function of the vertical ground force:

$$\sigma = K \gamma_{\text{soil}} d \quad (41)$$

Using this relation, the formula used for the shear force is:

$$\mathbf{fss} = A_{\text{shear}} K \gamma_{\text{soil}} d \tan(\phi_{\text{steel-soil}}) \quad (42)$$

For K the value 2 was taken. This value applies for piles driven into sand that densifies at the pile tip due to the driving vibrations. And finally, f_t is the force on the pad eye implied by the anchor line.

Neubecker and Randolph 1995 based their approach on the method of LeLievre and Tabatabaee 1981. They extended this method to incorporate:

- a more realistic 3-dimensional failure pattern in the soil,
- a force acting on the back of the fluke.

The latter modification is particularly important at shallow penetrations, when the bearing capacity of the anchor shank is insufficient to provide equilibrium (Figure 15).

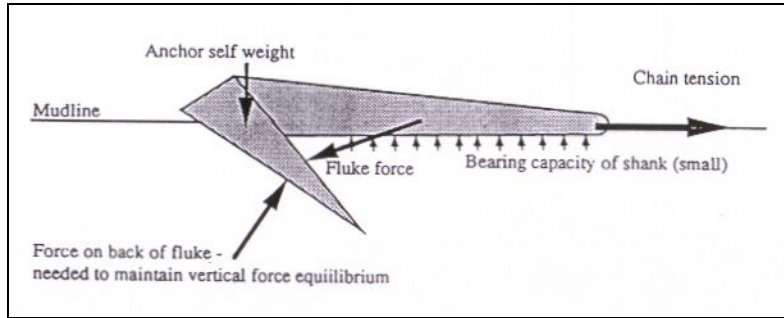


Figure 15: General force model

The authors suggested that the force on the shank is dependent on its size and shape and should be calculated from a bearing capacity viewpoint. Thus:

$$F_s = A_s \gamma d_s N_{qs} \quad (43)$$

The normal self-weight term ($\frac{1}{2} b \gamma N_\gamma$) is omitted in equation 44, because it is assumed to have a relatively small contribution and even the N_{qs} alone tends to over predict the shank resistance.

The 3-dimensional failure mode

Dickin 1988 presented an overview of some of the various methods that have been developed to evaluate the pullout resistance of a flat plate (Figure 16).

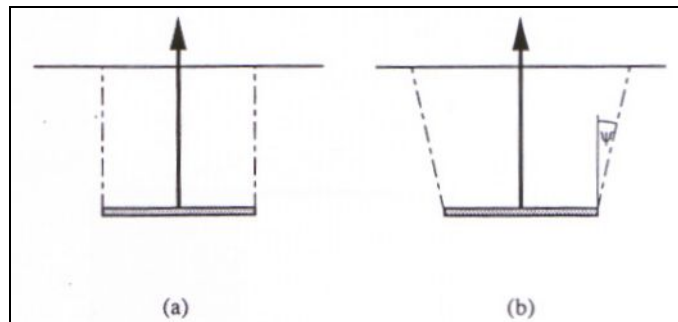


Figure 16. Slip surfaces used for flat plate pullout: (a) Majer 1955; (b) Vermeer and Sutjiadi 1985.

It was considered that the simple method of Majer (1955) consistently underestimated the pullout capacity of the flat plate, while the model of Vermeer and Sutjiadi (1985) gave predictions that compared well with observations. Neubecker and Randolph incorporated the model of Vermeer and Sutjiadi into the drag anchor problem as illustrated in Figure 17.

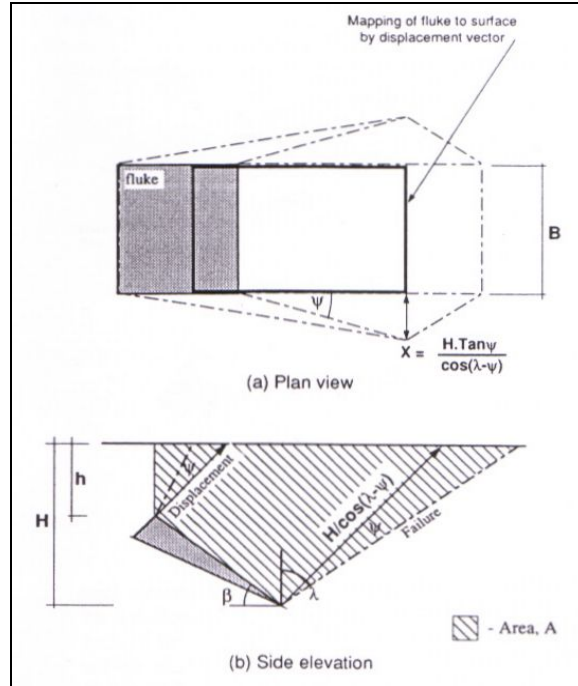


Figure 17. 3-dimensional failure mode.

The fluke can be thought of as being mapped onto the soil surface by the displacement vector of the soil wedge. The failure planes are inclined at the dilatation angle, ψ , to the displacement vector so that, when they reach the soil surface, the distance they are away from the fluke shadow is proportional to the depth of the original point. This 3-dimensional soil failure mode is still an idealized failure mode for the soil. However it does result in a more realistic description of the failure surface. The area, A , can be written as:

$$A = \frac{H^2 - h^2}{2 \tan \beta} + \frac{H^2 \tan \lambda}{2} \quad (44)$$

A simplification is made in the calculation of the cross-sectional area, A , in that a vertical slip surface is assumed behind the fluke, rather than an inclined one. This is supposed to have a minor effect on the balance of forces, as low active pressures are involved. However, no shear force is assumed across this surface and as such the extra soil mass included by this idealized failure mode counteracts the shear force that is neglected from the realistic failure mode.

The lateral extent of the failure wedge, X , is determined from simple geometry.

$$X = \frac{H \tan \psi}{\cos(\lambda - \psi)} \quad (45)$$

Using a pyramidal approximation for the sides of the wedge, the mobilized soil mass, W_s , is expressed as:

$$W_s = A \left(\gamma B + \frac{2}{3} \gamma X \right) \quad (46)$$

The side friction, SF , that is to be used in the limit equilibrium equations is obtained from Vermeer and Sutjiadi 1985.

$$SF = \frac{\gamma L(H+h)^2 (\sin \phi' - \sin \psi)}{4 \cos \psi (1 - \sin \phi' \sin \psi)} \quad (47)$$

Figure 18 and 19 show the system of forces with free body diagrams and force polygons for the soil wedge only, the anchor only and the combined anchor-soil body.

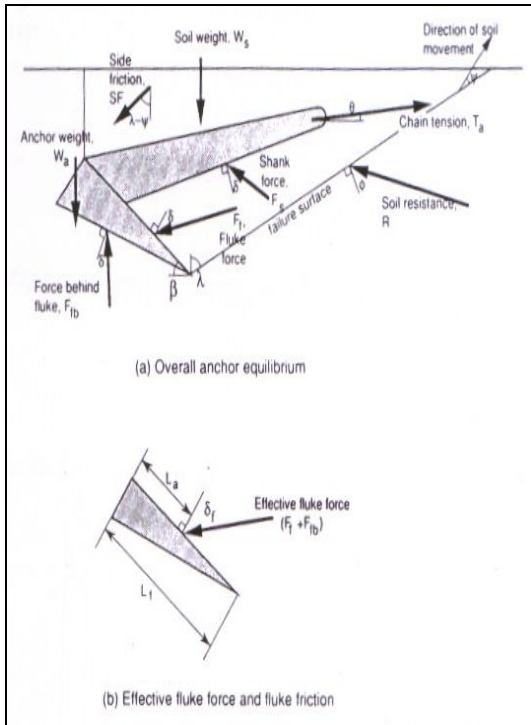


Figure 18. Free body diagram.

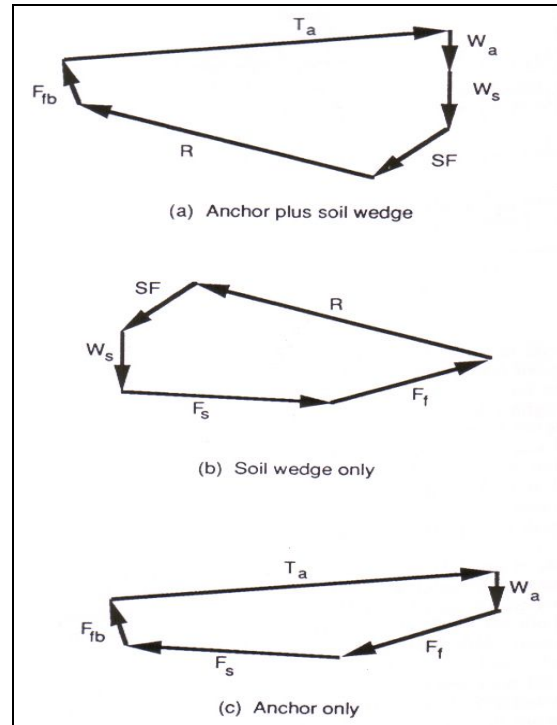


Figure 19. Force polygons.

The limit equilibrium calculation procedure is executed in the same way as that of Le Lievre and Tabatabaee 1981 in that the chain tension is calculated for a given failure wedge angle, λ , which is then varied until the chain tension reaches a minimum. The procedure begins however, by initially examining force equilibrium on the soil wedge only. The soil mass, W_s , and the side friction, SF , are calculated using equations 46 and 47, respectively, for the 3-dimensional soil wedge. The shank force, F_s , is calculated from the standard bearing capacity calculations from equation 43. The two unknown forces on the soil wedge, which are the fluke force, F_f , and the soil reaction, R , can be calculated from horizontal and vertical force equilibrium requirements. The force equilibrium of the anchor only is considered now. The fluke force, F_f , is defined from the previous equilibrium calculation, the weight of the anchor is known and the shank force, F_s , is calculated from equation 43. Again, there are only two unknown forces left for solution by force equilibrium, namely the force on the back of the fluke, F_{fb} , and the chain tension, T_a . The failure wedge angle, λ , is then varied and the process repeated to obtain a minimum upper bound estimate of T_a . The solution of this force system still proceeds using simple limit equilibrium methods, however, the equilibrium solution is applied in a two step manner to arrive at a chain load and the introduction of an extra unknown and an extra equation has resulted in a more realistic force system acting on the anchor.

Finally the American Petroleum Institute 2005 gives a graph for the holding capacity in sand based on the ratio of the weight of the anchor and the holding capacity. This graph is shown in Figure 20, and gives lines for different types of anchors.

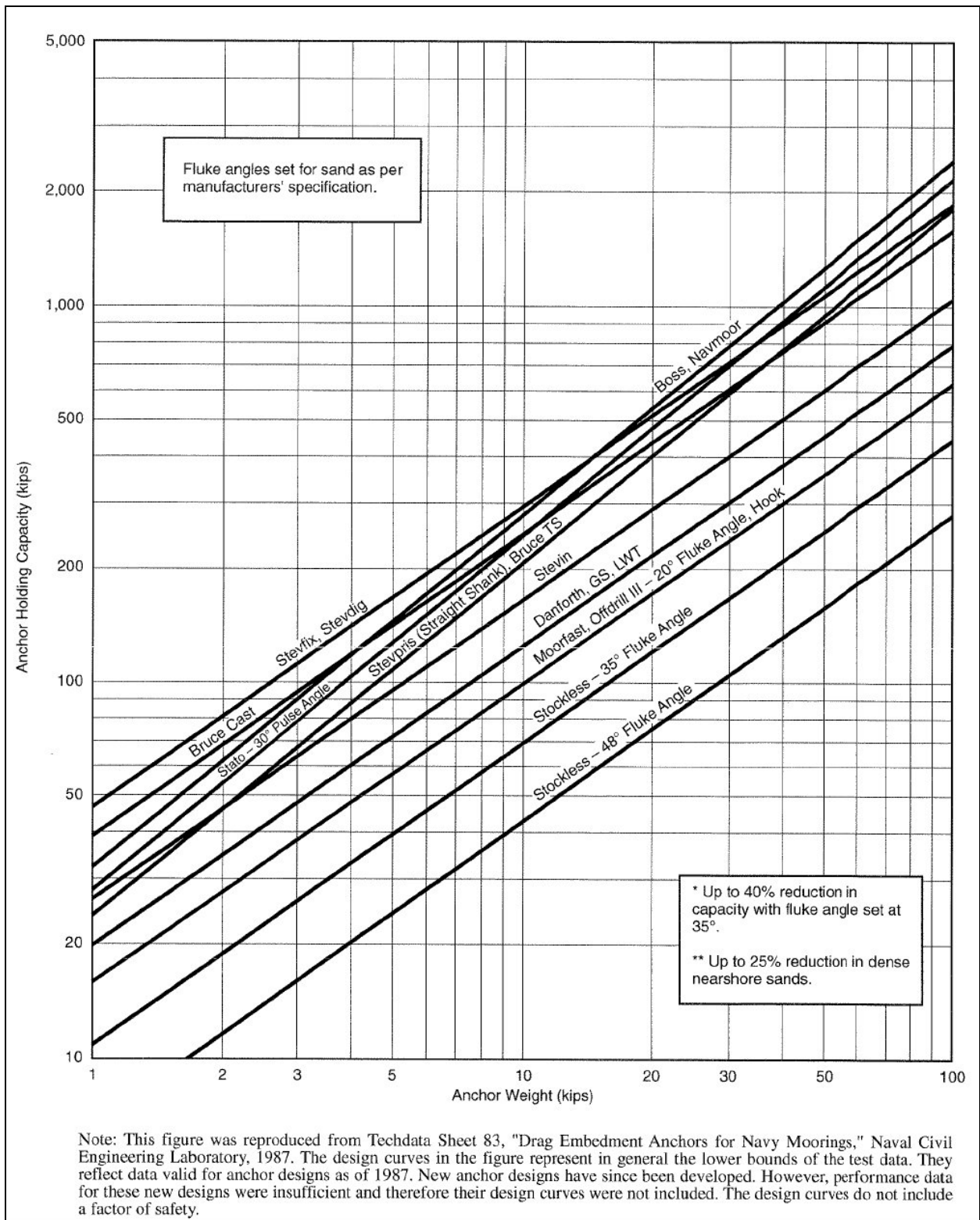


Figure 20. Anchor holding capacity in sand (API 2005).

Miedema et al 2006 derived a model based on 4 different penetration phases. The model is described below.

PENETRATION PHASES

Phase 1: No penetration

In this first situation the anchor lies on the bed of soil and the fluke/shank angle will be considered as a minimum. When pulling on the mooring line the anchor will scratch over the seabed, see Figure 21. A bed of soil will be formed in front of the fluke and will give some resistance. Because of this resistance, an angle κ will reach its maximum at a certain point. At that certain point, the bed of soil in front of the fluke will give his highest resistance and it will become easier to penetrate than scratching over the seabed. When the assumption of a perfect sharp fluke point is made, the point load can be neglected.

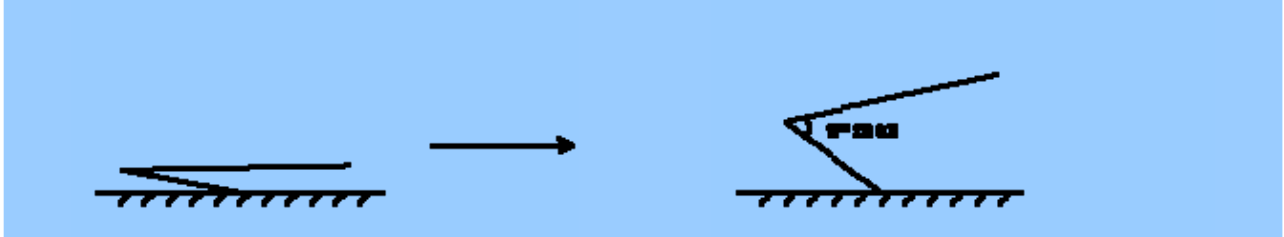


Figure 21. The anchor on top of the soil in phase 1.

Phase 2: Penetration causes fluke forces

When the fluke starts to penetrate (Figures 22 and 23), the cutting theory of Miedema 1987, can be used. Forces that will play a role in the force balance are the fluke forces. When the angles on the fluke are considered, a few assumptions can be made. First of all the fluke/shank angle κ will be constant and will have its maximum value. The internal friction and the external friction angles are also constant. These parameters are only depending on the material of the anchor and soil mechanical properties.

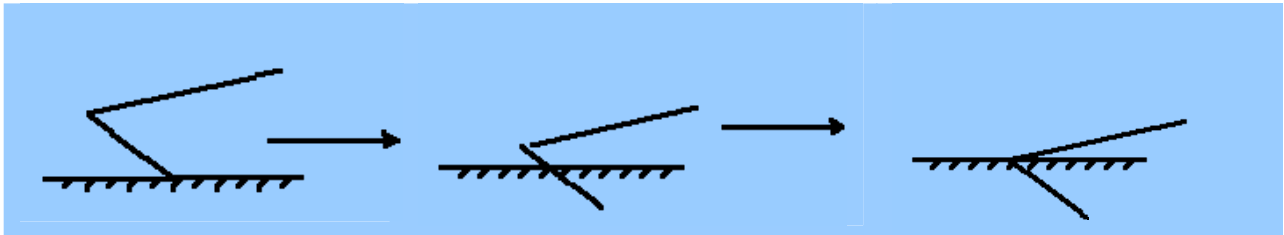


Figure 22. The fluke penetrating the soil in phase 2.

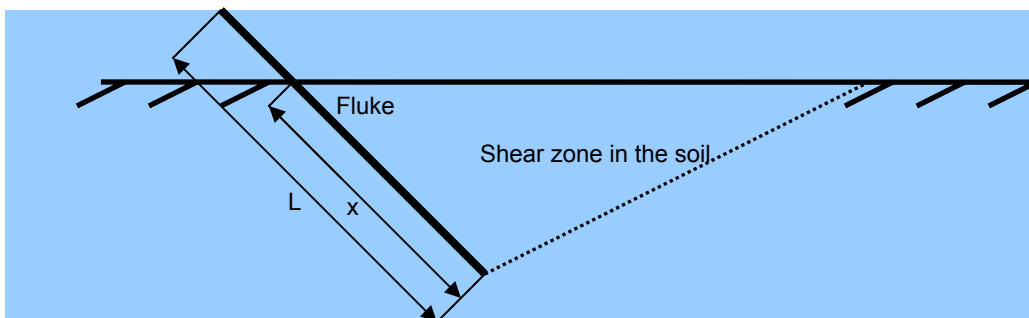


Figure 23. The fluke in the soil.

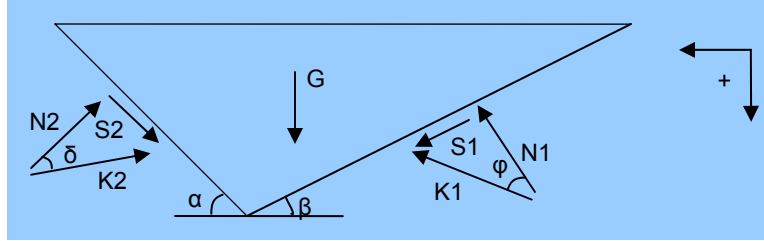


Figure 24. The forces on the soil layer.

As discussed before the cohesion, adhesion, inertial forces and water tension can be neglected. According to Figures 24 and 28, a force balance can be calculated.

The shear force and the normal force are related according:

$$S_1 = N_1 \tan \varphi \quad (48)$$

$$S_2 = N_2 \tan \delta \quad (49)$$

The grain forces will be:

$$K_1 = \sqrt{(S_1^2 + N_1^2)} \quad (50)$$

$$K_2 = \sqrt{(S_2^2 + N_2^2)} \quad (51)$$

The weight of the soil can be given as a force according:

$$G = \left(\frac{x^2 \sin^2 \alpha}{2 \tan \alpha} + \frac{x^2 \sin^2 \alpha}{2 \tan \beta} \right) \cdot \gamma \quad (52)$$

Horizontal equilibrium of forces:

$$K_1 \cdot \sin(\beta + \varphi) - K_2 \cdot \sin(\alpha + \delta) = 0 \quad (53)$$

Vertical equilibrium of forces:

$$-K_1 \cdot \cos(\beta + \varphi) + G - K_2 \cdot \cos(\alpha + \delta) = 0 \quad (54)$$

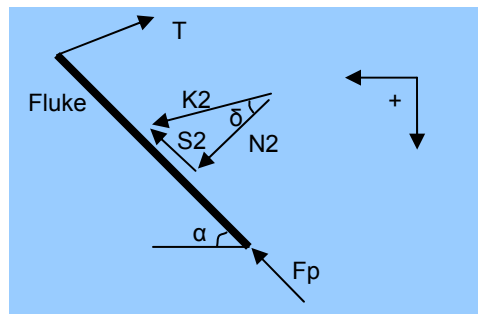


Figure 25. The forces on the fluke.

The force K_2 on the fluke is important to determine the horizontal and vertical acting forces on the fluke (Figure 25).

$$K_2 = \frac{G \cdot \sin(\beta + \varphi)}{\sin(\alpha + \beta + \varphi + \delta)} \quad (55)$$

The following forces are acting on the fluke blade:

- The Horizontal Force

$$F_h = K_2 \cdot \sin(\alpha + \delta) \quad (56)$$

- The Vertical Force

$$F_v = K_2 \cdot \cos(\alpha + \delta) \quad (57)$$

The force F_p can be neglected as discussed before.

Phase 3: Penetration causes fluke and shank forces

In this situation the fluke is completely covered by sand and the shank will become an extra factor which will cause penetration resistance, see Figures 26 and 27. For the shank the cutting theory of Miedema 1987, can't be used. The strip footing theory, as described in Verruijt (2000), will be used for determining the shank resistance. The maximum shank resistance acts when the complete shank is penetrated.



Figure 26. The shank penetrating the soil in phase 3.

In this paragraph you will find the modeling of the forces on the fluke and the shank. The influences of the angles will be given. The cutting theory of Miedema (1987) is still valid for the fluke part of the anchor forces. For determining the forces on the shank, the strip footing theory, as described in Verruijt (2000), will be used. For phase 3, two shear zones are taken into account. This will lead to a geometry as shown in Figure 28.

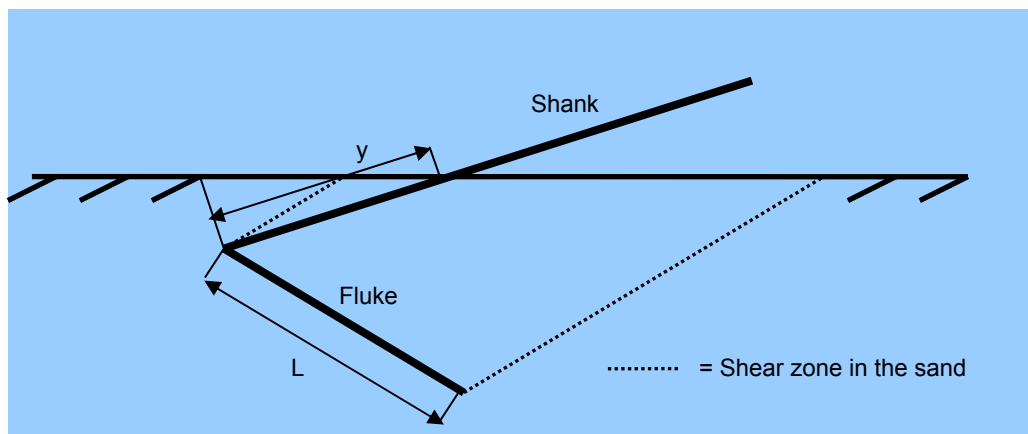


Figure 27. The fluke and shank in the soil.

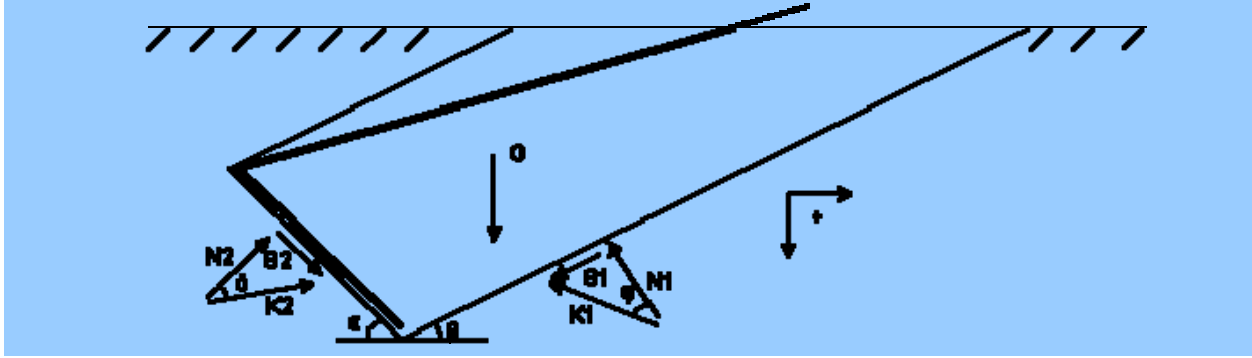


Figure 28. Forces on the soil layer.

As discussed before; the cohesion, adhesion, inertial forces and water tension can be neglected. For the Figures 28 and 30, a force balance can be calculated. The shear force and the normal force are related according:

The shear force and the normal force are related according:

$$S_1 = N_1 \tan \varphi \quad (58)$$

$$S_2 = N_2 \tan \delta \quad (59)$$

The grain forces will be:

$$K_1 = \sqrt{(S_1^2 + N_1^2)} \quad (60)$$

$$K_2 = \sqrt{(S_2^2 + N_2^2)} \quad (61)$$

The weight of the soil can be determined by using the geometry of Figure 29, so the weight of the soil will be:

$$G = A_{\square} \cdot \gamma \quad (62)$$

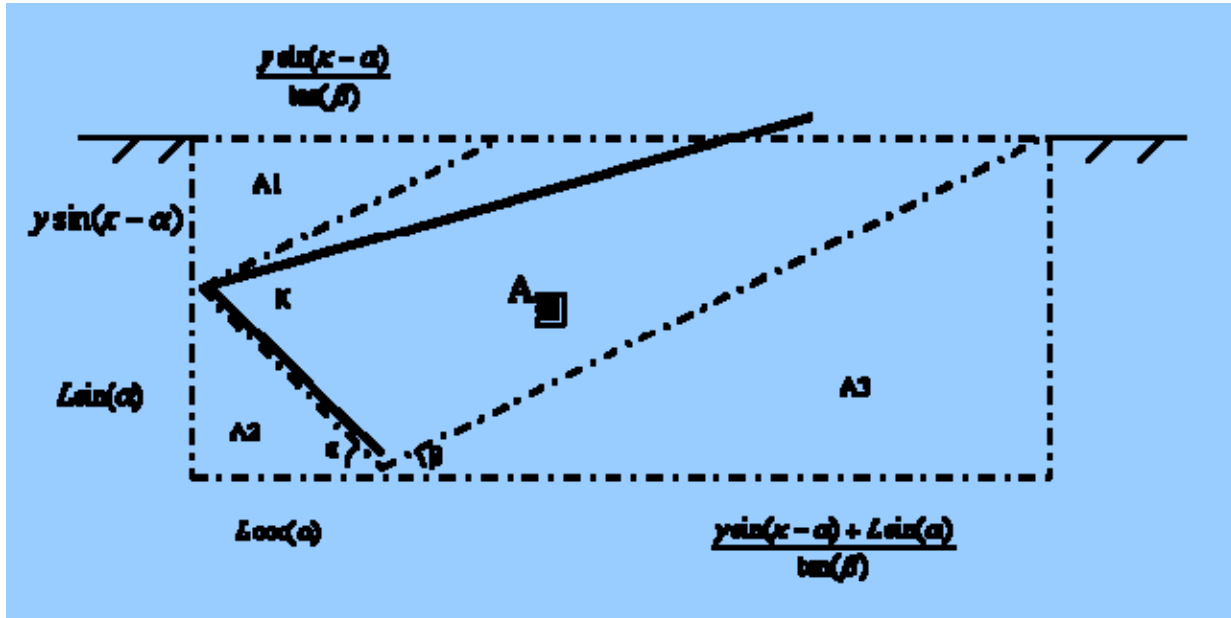


Figure 29. The dimensions of the soil layer.

with:

$$A_{\text{fluke}} := (y \cdot \sin(\kappa - \alpha) + L \cdot \sin(\alpha)) \cdot \left(L \cdot \cos(\alpha) + \frac{y \cdot \sin(\kappa - \alpha) + L \cdot \sin(\alpha)}{\tan(\beta)} \right) - \left(\frac{y^2 \cdot \sin(\kappa - \alpha)}{2 \cdot \tan(\beta)} \right) - \frac{1}{2} \cdot L^2 \cdot \sin(\alpha) \cdot \cos(\alpha) - \left(\frac{(y \cdot \sin(\kappa - \alpha) + L \cdot \sin(\alpha))^2}{2 \cdot \tan(\beta)} \right) \quad (63)$$

Forces on the fluke and the shank

For the determination of the forces on the fluke and the shank, Figure 30, two different theories will be used. For the fluke the cutting theory of Miedema is valid, therefore forces on the soil layer and on the fluke are the same as discussed in phase 2. For the forces on the shank the strip footing theory can be used. This theory is based on the fundamentals of Brinch Hansen and is a generalization of the Prantl theory. This can be found in Verruijt 2000.

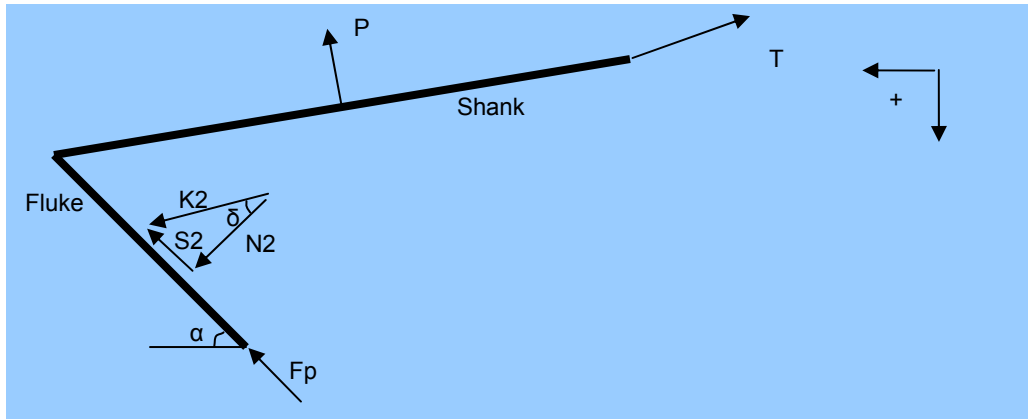


Figure 30. The forces on the anchor.

To determine the friction Brinch Hansen force P on the shank we can make use of:

$$P = i_c s_c c N_c + i_q s_q q N_q + i_\gamma s_\gamma \frac{1}{2} \gamma B N_\gamma \quad (64)$$

Where c is cohesion and q is the external load on the soil

Because c and q are zero in this case (no cohesion and no external force on the soil), P will only be a function of the soil weight part of the function, so:

$$P = i_\gamma s_\gamma \frac{1}{2} \gamma B N_\gamma \quad (65)$$

Hereby i_γ is a correction factor for inclination factors of the load. The factor s_γ is a shape factor for the shape of the load.

In this case, only a load perpendicular to the soil will be considered, so i_γ will be removed from the formula.

Inserting N_γ :

$$P = \left(1 - 0,3 \frac{B}{y}\right) B^2 y \gamma \left(\frac{1 + \sin \phi}{1 - \sin \phi} e^{\pi \tan \phi} - 1\right) \tan \phi \quad (66)$$

Now the friction part of the shank has to be determined. For the friction of the shank, the next formula is valid:

$$F_{\text{friction}} = \sigma_n \tan(\delta) y h \quad (67)$$

It is possible now to plot the results for P and F_{friction} (see Figure 31) then it is possible to find out if the downward force of the fluke is big enough to pull the shank through the seabed and further.

It is also possible now to make a total force and moment balance, to predict the trajectory of the anchor.

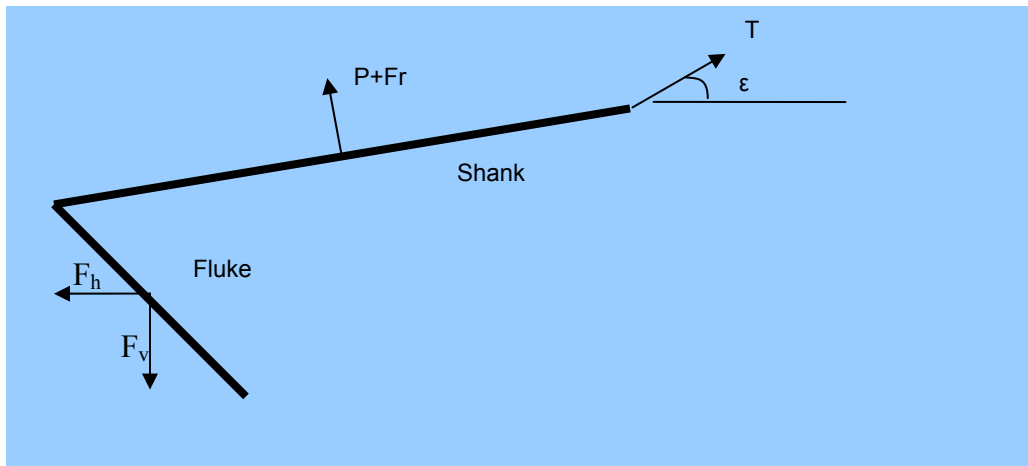


Figure 31. The forces on the anchor.

Phase 4: Penetration causes fluke forces, shank forces and mooring line forces



Figure 32. The mooring line penetrating the soil in phase 4.

The fluke and the shank are completely covered by sand (Figures 32 and 33). When there is still no equilibrium, a part of the mooring line will enter the soil. The mooring line penetration will lead to an extra factor which will cause penetration resistance. The anchor becomes stable when there is a balance between the vertical and horizontal forces on the anchor part, which is covered by sand.

In this phase you will find the modeling of the forces on the fluke, the shank and the mooring line. The cutting theory of Miedema is still valid for the fluke part of the anchor forces. For determining the forces on the shank and the mooring line we will use the strip footing theory as discussed in Verruijt.

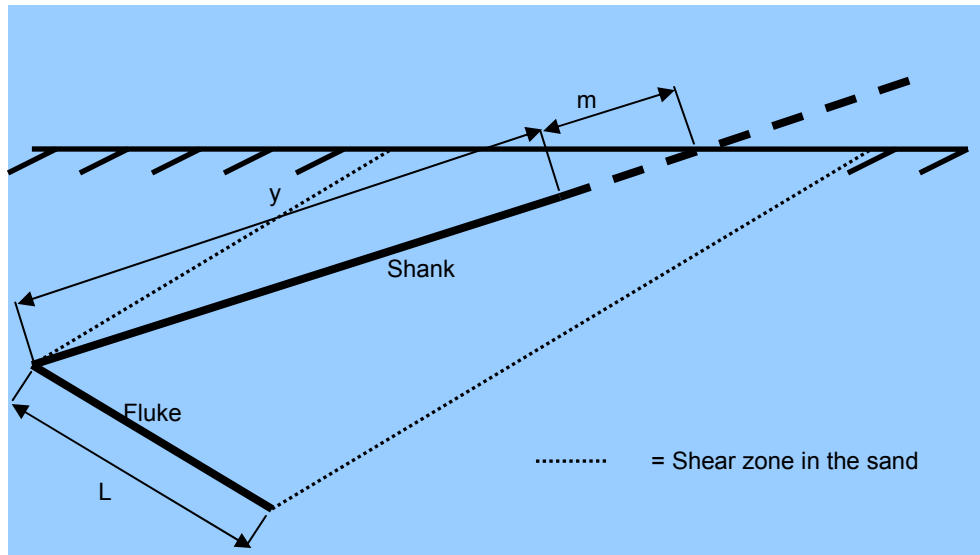


Figure 33. Fluke, shank and mooring line in the soil.

The soil layer properties can be interpreted in a same way as described in phase 3. So this way the function for G is still valid.

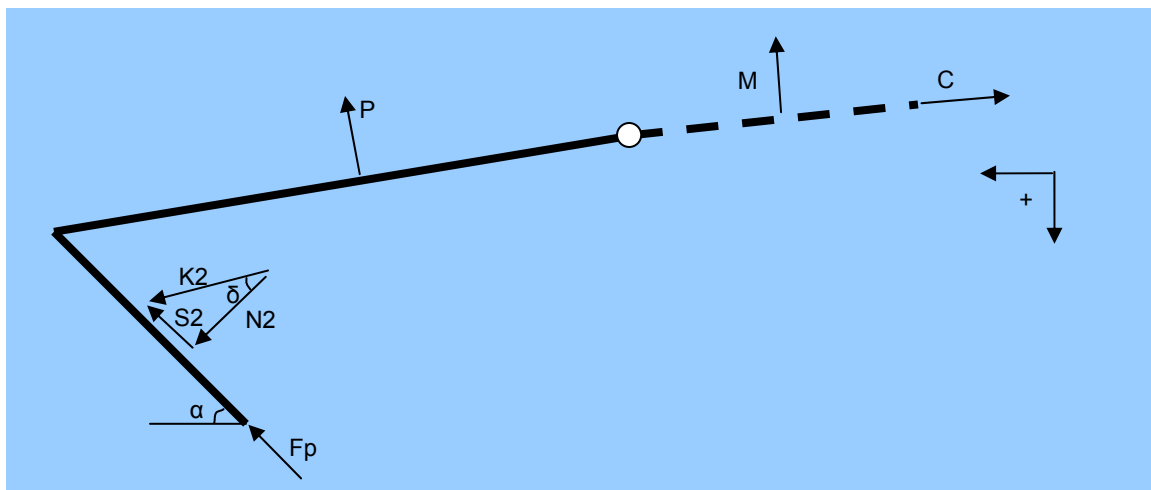


Figure 34. Forces on the fluke, shank and mooring line.

To determine the forces on the anchor for this situation the theory as discussed in phase 3 is valid. For the mooring line forces (Figures 34 and 35) we will also use the Brinch Hansen theory as discussed in Verruijt 2000.

The penetration of the mooring line causes resistance perpendicular to this line (penetration resistance, see Figure 36). This effect is noticeable in all soil conditions. The type of mooring line will determine the value of this resistance. Think of a wire rope mooring line which penetrates deeper (less resistance) than a chain mooring line. During the penetration process of the anchor, the resistance increases when depth increases, which is related to the position of the anchor.

The mooring line penetration can be described by the following geometry: When looking at the point where the anchor becomes stable, a force and moment balance can be made out of all the forces on the anchor and mooring line. In fact this is the moment where the anchor reaches his maximum holding capacity.

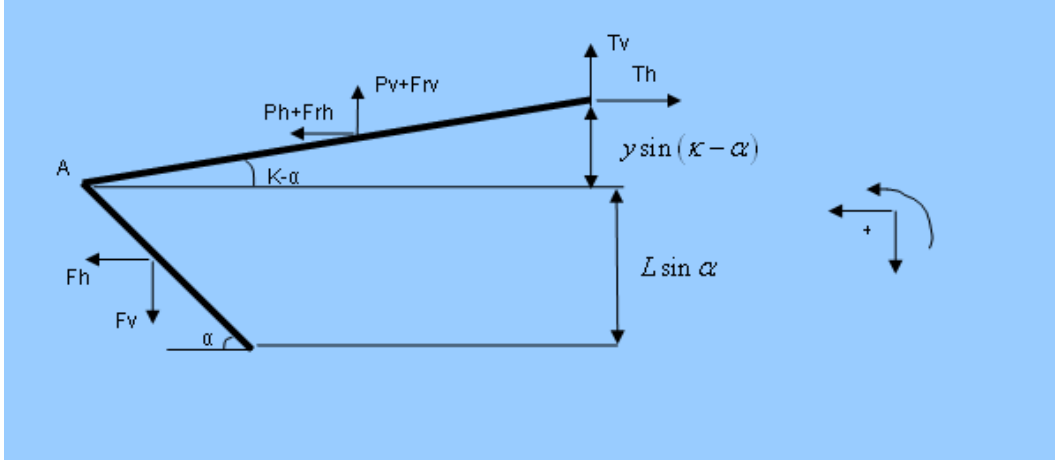


Figure 35. The forces on the anchor.

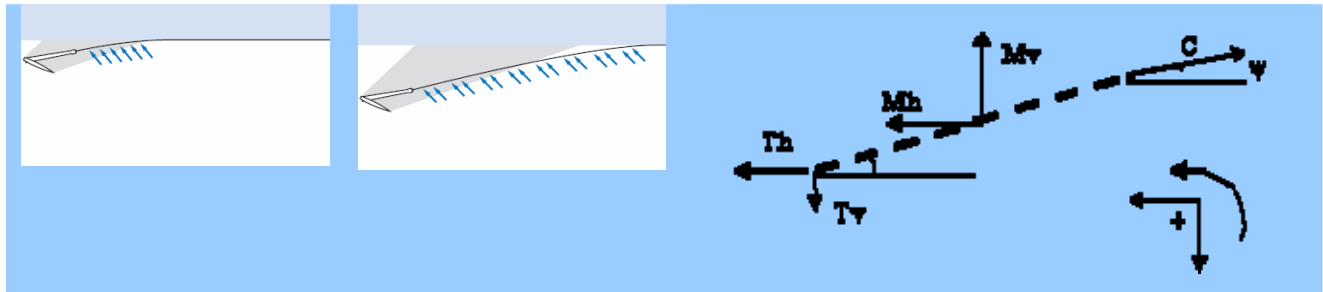


Figure 36. The forces on the mooring line.

Vertical equilibrium of forces:

$$F_v - P_v - F_{rv} - M_v - T_v = 0 \quad (68)$$

Horizontal equilibrium of forces:

$$F_h + P_h + F_{rh} + M_h - T_h = 0 \quad (69)$$

Moment balance to point A:

$$\begin{aligned} -F_v \cdot \frac{1}{2} L \cos \alpha - F_h \cdot \frac{1}{2} L \sin \alpha + (P_v + F_{rv}) \cdot \frac{1}{2} y \cos(\kappa - \alpha) + (P_h + F_{rh}) \cdot \frac{1}{2} y \sin(\kappa - \alpha) \\ + T_v \cdot y \cos(\kappa - \alpha) + T_h \cdot y \sin(\kappa - \alpha) = 0 \end{aligned} \quad (70)$$

CONCLUSIONS AND RECOMMENDATIONS

In the penetration behavior the different forces and moments in all four phases can be described with the theory dealt with, in this document. These forces and moments are a function of the anchor geometry. The holding capacity of the anchor is described as well as a function of the depth and the geometry. To predict the trajectory of the anchor during the penetration, one has to find a relationship between the different forces and moments on the anchor and the trajectory of the anchor. The anchor trajectory will stop when the different forces are in equilibrium, or when the pull force will be too high for that particular anchor, at a certain depth. In the last case, the pull force necessary to penetrate deeper in the soil, is higher then the maximum holding capacity of that particular anchor at a certain depth. to that point the maximum holding capacity is reached (see Figure 37). When pulling further, the anchor will be pulled out and loses his function.

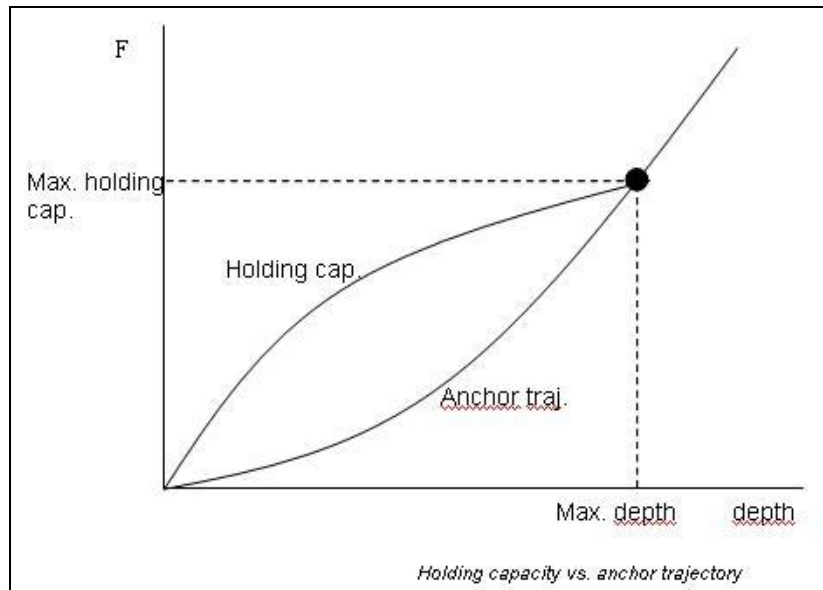


Figure 37. Holding capacity vs. anchor trajectory.

LIST OF SYMBOLS USED

A_s	The area of the shank	m^2
B	Width of the shank	m
B_s	The effective chain width in sliding	m
B_b	The width of the footing, which is the chain width in bearing	m
c	Cohesion	kPa
C	Catenary force	kN
d	Depth of bottom footing	m
D	the pad eye embedment depth	m
f	Anchor form factor	-
f	soil frictional resistance per unit chain length	kN/m
h	Height of the shank	m
h	the depth of the footing.	m
L	Total fluke length	m
M	Resistance on mooring line	kN/m
N_c	Baring-capacity factor for clay	-
N_γ	Bearing capacity factor	-
N_q	Bearing capacity factor	-
p	soil normal/bearing resistance per unit chain length	kN/m
q	the normal ultimate soil pressure	kPa
Q	the average bearing resistance of the chain in the soil	kN
S_u	the undrained shear strength of the soil	kPa
Δs	chain element length	m
T	Anchor pull force	kN
T_a	the chain load at the anchor pad eye	kN
T_0	the chain load at the seabed	kN
T_1	chain tension at the top of the chain element	kN
T_2	chain tension at the bottom of the chain element	kN
w	effective chain weight in soil per unit chain length	kg/m
y	Length of the shank in the sand	m
z	Depth	m
α	Angle of the fluke in the sand	rad
β	Angle of the shear zone, inclination fluke	rad
φ	Internal friction angle of the sand	rad
δ	External friction angle fluke/sand	rad
χ	Length of the fluke in the sand	m
γ	Density of the in situ sand	ton/m^3
κ	Angle between fluke and shank	rad
φ	Internal friction angle sand	rad
μ	the friction coefficient between the chain and soil	-
α	a reduction factor (= 1 for soft clay)	-
σ_n	Normal stress on the area of the shank	N/m^2
Φ_1	chain angle at the top of the chain element	rad
Φ_2	chain angle at the bottom of the chain element	rad
θ_a	the chain angle at the anchor padeye	rad
λ	Failure wedge angle	rad

REFERENCES

- API (American Petroleum Institute) 2005, "Design and analysis of stationkeeping systems for floating structures". Recommended practice 2SK 2005.
- Degenkamp, G. and Dutta, A., 1989. "Behaviour of Embedded Mooring Chains in Clay During Chain Tensioning." Offshore Technology Conference, Paper 6031.
- Degenkamp, G. and Dutta, A., 1989. "Soil Resistances to Embedded Anchor Chain in Soft Clay." Journal of Geotechnical Engineering Vol 115, No. 10
- Det Norske Veritas., 2002. "Design and Installation of Plate Anchors in Clay." Recommended Practice DNV-RP-302.
- Dunnivant, T.W. and Kwan, C-T.T., 1993. "Centrifuge Modeling and Parametric Analysis of Drag Anchor Behavior." Offshore Technology Conference, Paper OTC 7202.
- Grote, B.J.H., 1993. "Simulation of Kinematic Behavior of Workanchors." Faculty of Mechanical Engineering, Offshore Engineering Major, Report nr: 92.3.GV.3034, 93.3.GV.4074 and 93.3.GV.4167, Delft University of Technology.
- House, A., 1998. "Drag Anchor and Chain Performance in Stratified Soils." Geomechanics Group, Report 1319, The University of Western Australia.
- Lammes, R.R. and Siemers, R.W., 1988. "Soil Mechanics of Drag Embedment Anchor in Sand." Faculty of Civil Engineering, Offshore Engineering Major, Delft University of Technology.
- Lin, K. and Randolph, M.F., 1998. "Numerical Analysis of Stresses and Displacements in Layered Soil Systems." Geomechanics Group, Report G1334, The University of Western Australia.
- Miedema, S.A., 1987, "Calculation of the Cutting Forces when Cutting Water Saturated Sand". Ph.D. Thesis, Delft University of Technology, September 15th 1987.
- Miedema, S.A. , Kerkvliet, J., Srijbis, D., Jonkman, B., Hatert, M. v/d, 2006, "THE DIGGING AND HOLDING CAPACITY OF ANCHORS". WEDA XXVI AND TAMU 38, San Diego, California, June 25-28.
- Mierlo, R. v., 2005. "Anchor Trajectory Modeling." Faculty of Mechanical Engineering, Offshore Engineering Major, Delft University of Technology.
- Murff, J.D., Randolph, M.F. & Elkhatab, S., Kolk, H.J., Ruinen, R.M., Strom, P.J. and Thorne, C.P., 2005. "Vertically Loaded Plate Anchors for Deepwater Applications." Frontiers in Offshore Geotechnics ISFOG.
- Ruinen, R.M., 2005. "Influence of Anchor Geometry and Soil Properties on Numerical Modeling of Drag Anchor Behavior in Soft Clay." Frontiers in Offshore Geotechnics ISFOG.
- Neubecker, S.R. and Randolph, M.F., 1996. "The Static Equilibrium of Drag Anchors in Sand." Canadian Geotechnical Journal 33: 574-583
- Neubecker, S.R. and Randolph, M.F., 1996. "The Kinematic Behavior of Drag Anchors in Sand." Canadian Geotechnical Journal 33: 584-594
- Neubecker, S.R. and Randolph, M.F., 1995. "Performance of Embedded Anchor Chains and Consequences for Anchor Design." Offshore Technology Conference, Paper OTC 7712.
- Neubecker, S.R. and Randolph, M.F., 1995. "Profile and Frictional Capacity of Embedded Anchor Chains." Journal of Geotechnical Engineering Vol. 121, No. 11
- Neubecker, S.R. and Randolph, M.F., 1995. "The Performance of Drag Anchor and Chain Systems in Cohesive Soil." Geomechanics Group, Report G1168, The University of Western Australia.
- Neubecker, S.R. and Randolph, M.F., 1994. "Profile and Frictional Capacity of Embedded Anchor Chains." Geomechanics Group, Report G1142, The University of Western Australia.
- O'Neill, M.P. and Randolph, M.F., 1998. "The Behaviour of Drag Anchors in Layered Calcareous Soils." Geomechanics Group, Report G1329, The University of Western Australia.
- O'Neill, M.P., Randolph, M.F. and House, A.R., 1998. "The Behaviour of Drag Anchors in Layered Soils." Geomechanics Group, Report G1346, The University of Western Australia.
- Stewart, W.P., 1992. "Drag Embedment Anchor Performance Prediction in Soft Soils." Offshore Technology Conference, Paper OTC 6970.
- Thorne, C.P., 1998. "Penetration and Load Capacity of Marine Drag Anchors in Soft Clay."
- Verruijt, A., "Soil Mechanics". Lecture Notes, Delft University of Technology, 2000.
- Vrijhof Anchors, 2005, "Anchor manual 2005"

